Memorandum
Vol. 7, No. 4 / April 2020 / Optica 333

optica

Sub-wavelength GHz-fast broadband ITO Mach–Zehnder modulator on silicon photonics

Rubab Amin,[1] Rishi Maiti,[1] Yaliang Gui,[1] Can Suer,[1] Mario Miscuglio,[1] Elham Heidari,[2] Ray T. Chen,[2] Hamed Dalir,[3] and Volker J. Sorger[1,*]

[1]Department of Electrical and Computer Engineering, George Washington University, Washington, DC 20052, USA
[2]Microelectronics Research Center, Electrical and Computer Engineering Department, University of Texas at Austin, Austin, Texas 78758, USA
[3]Omega Optics, Inc., 8500 Shoal Creek Blvd., Bldg. 4, Suite 200, Austin, Texas 78757, USA
*Corresponding author: sorger@gwu.edu

Received 30 January 2020; revised 23 February 2020; accepted 16 March 2020 (Doc. ID 389437); published 13 April 2020

Here we demonstrate a spectrally broadband, gigahertz-fast Mach–Zehnder interferometric modulator exhibiting a miniscule $V_{\pi}L$ of 95 $V \cdot \mu m$, deploying a subwavelength short electrostatically tunable plasmonic phase shifter based on heterogeneously integrated indium tin oxide thin films into silicon photonics.

https://doi.org/10.1364/OPTICA.389437

Indium tin oxide (ITO), belonging to the class of transparent conductive oxides, is a material extensively adopted in high-tech industry such as in touchscreen displays of smartphones or contacts for solar cells. Recently, ITO has been explored for electro-optic modulation using its free-carrier dispersive effect enabling unity-strong index modulation [1–3]. However, gigahertz (GHz)-fast modulation capability using ITO is yet to be demonstrated—a feature we show herein. Given the ubiquitous usage of phase-shifter (PS) technologies, such as in data communication, optical phased arrays, analog and RF photonics, sensing, and so on, here we focus on a Mach–Zehnder interferometer (MZI)-based modulator to demonstrate a comprehensive platform of heterogeneous integration of ITO-based opto-electronics into silicon photonic integrated circuits (PIC). Since the real part of the optical refractive index (n) is of interest in PSs, in previous studies we have shown the interplay between a selected optical mode (e.g., photonic bulk versus plasmonic) and the material's figure of merit ($\Delta n/\Delta\alpha$), where α is the optical loss, directly resultant from Kramers–Kronig relations [4]. Additionally, ITO can be selectively prepared (via process conditions [5]) for operating in either an n-dominant or α-dominated region [4], demonstrating a photonic-mode ITO-oxide-Si MZI on silicon photonics with an efficient $V_{\pi}L = 0.52\ V \cdot mm$ [2] and a plasmonic version deploying a lateral gate exhibiting a $V_{\pi}L = 0.063\ V \cdot mm$ [6]. Indeed, a plasmonic mode enables a strong light–matter interaction (e.g., extrinsic slow-light effect), which, when superimposed with ITO's intrinsic slow-light effect, proximal epsilon-near-zero (ENZ) effects [7], enables realization of just 1–3 μm short PSs [4], allowing small (~fF) electrical capacitances for efficient and fast signal modulation. Here we design the ITO material parameters to control operation in the n-dominant region adequately close to but not at the high-loss ENZ (ENZ located in the α-dominant region) [4]. In fact, unlike lithium niobate (LN) optoelectronics requiring careful crystal-orientation control [8,9], ITO thin films are crystal-orientation independent and feature intrinsically uniform optical characteristics as deposited. Here we discuss an ITO-plasmon-based PS heterogeneously integrated into a silicon photonic MZI delivering GHz-fast broadband modulation and thus open opportunities for multispectral operation.

The base interferometer is taped out as a symmetric silicon-on-insulator (SOI) MZI to minimize chirp effects induced by different splitting ratios in the Y junctions of the MZI and includes post-tape out loss balancing between both arms using a metallic strip (L_b) on the nonmodulated arm to minimize extinction ratio (ER) degradation [Fig. 1(a)]. Sweep of the active PS device length (L_d) ranges from sub-λ (1.4 μm) to λ-scale devices (3.5 μm) [Fig. 1(b)]. Broadband spectral response is measured in the C band [~30 nm, Fig. 2(a)], which is expected since the plasmonic resonance of the mode has a FWHM ~100s of nanometers (nm). The spectral response is determined by ITO dispersion and

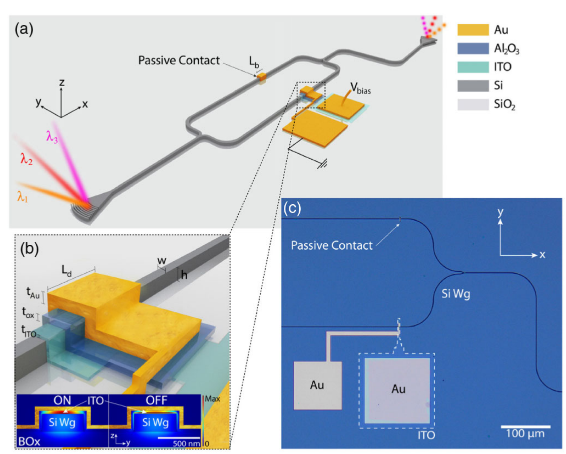

Fig. 1. (a) Schematic of the broadband GHz plasmonic ITO-based Mach–Zehnder modulator; (b) active device region, L_d; $t_{Au} = 50$ nm, $t_{ox} = 20$ nm, $t_{ITO} = 10$ nm, $w = 500$ nm, $h = 220$ nm; corresponding FEM eigenmode profiles to light ON and OFF states (inset); (c) optical microscope image of the sub-λ ($L_d = 1.4$ μm) modulator.

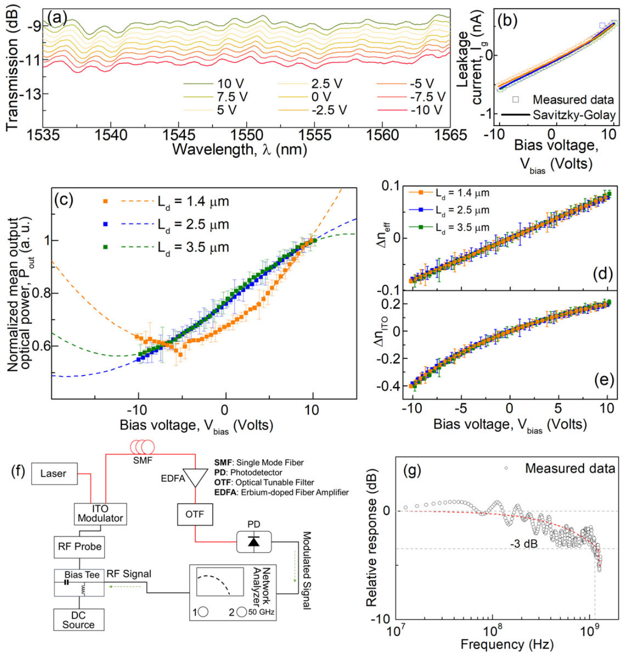

Fig. 2. (a) Optical transmission exhibiting broadband performance of the modulator; (b) I-V measurements; (c) optical output modulation under DC bias for different device scaling, where dashed lines represent $\cos^2(\text{arg})$ fit dictated by Mach–Zehnder operating principle; (d) induced effective index change Δn_{eff} and (e) ITO material index change Δn_{ITO} from applied bias; (f) experimental speed setup; and (g) measured small-signal response S_{21} of the modulator.

proximity to the ENZ. For ultrabroadband applications (e.g., 100+ nm) ITO modulators for different spectral regions (e.g., $\Delta\lambda = 50$ nm) can be processed using different conditions [5]. Functional capacitor traits in the measured bias range are observed [Fig. 2(b)]. DC electro-optic transmission power tests and squared cosine fit (as dictated by MZI operating principle) result in an ER of ∼3 to > 8dB, respectively [Fig. 2(c)]. The measured $V_\pi L$ is just 95 ± 2 V · μm and rather constant across all device scaling. The results indicate a modal index change Δn_{eff} of ∼0.2 [Fig. 2(d)], and FEM eigenmode analysis [inset, Fig. 1(b)] reveals an ITO index change of about 0.6 [Fig. 2(e)] reflecting an ∼2× increased confinement factor (Γ) corresponding to active biasing, slightly lower than previous ITO modulators [2], and intentionally enabling lower insertion loss (IL) of about 6.7 dB. Cutback measurements reveal 1.6 dB/μm propagation loss in the active region and an additional 1.3 dB/coupling loss from in/out coupling of the mode from the Si waveguide, while the passive loss balancing contact [Fig. 1(a), L_b] exhibits a 1.2 dB/μm propagation loss and 1.1 dB/coupling loss, correspondingly. Note that the high loss per unit length in plasmonics is alleviated by an enhanced light–matter interaction enabling λ-short device lengths (L_d); thus the total IL is comparable to Si photonic MZIs. The deposited ITO thin film carrier concentration N_c of 3.1×10^{20} cm^{-3} is determined from metrology, and a change $\Delta N_c = 2.1 \times 10^{20}$ cm^{-3} estimated from the gated measurements suggests n-dominant operation, however intentionally away from the high-loss ENZ ($6 - 7 \times 10^{20}$ cm^{-3}) state, yet sufficiently near to capture a slow-light effect [4].

Frequency response (S_{21}) is obtained by generating a low power modulating signal (0 dBm) with a 50 GHz network analyzer; a bias tee combines DC voltage (6 V) with the RF signal [Fig. 2(f)]. RF output from the modulator is amplified using a broadband erbium-doped fiber amplifier (EDFA, ∼35 dB), and an optical tunable filter reduces undesired noise by 20 dB. The modulated light is collected by a photodetector. The −3 dB roll-off (small signal) shows a speed of 1.1 GHz [Fig. 2(g)], which matches estimations for the RC delay given capacitance of 213 fF and total resistance of 680 Ω, while dynamic switching energy (∼pJ) characterizes the spectral trade-off [2]. Performance comparison of this ITO paradigm with recent modulators shows similar achievable speeds, allowing for CMOS low drive voltages and competent $V_\pi L$ enabled by efficient electrostatics ($t_{\text{ox}} = 5$ nm, Hf_3N_4, pad-overlay optimization, annealing, plasma treatment), which is fundamentally challenging in LN due to its delicate loss sensitivity (Table 1).

This GHz-fast broadband integrated modulator bears relevance since ITO is a foundry-compatible material. Unlike the crystal-orientation-sensitive LN, ITO optoelectronics is synergistic to enhancing electrostatics known from transistor technology.

Funding. Air Force Office of Scientific Research (FA9550-17-1-0071, FA9550-17-1-0377).

Disclosures. The authors declare no conflicts of interest.

REFERENCES

1. V. J. Sorger, N. D. Lanzillotti- Kimura, R. Ma, and X. Zhang, Nanophotonics **1**, 17 (2012).
2. R. Amin, R. Maiti, C. Carfano, Z. Ma, M. H. Tahersima, Y. Lilach, D. Ratnayake, H. Dalir, and V. J. Sorger, APL Photon. **3**, 126104 (2018).
3. E. Li, Q. Gao, S. Liverman, and A. X. Wang, Opt. Lett. **43**, 4429 (2018).
4. R. Amin, C. Suer, Z. Ma, I. Sarpkaya, J. B. Khurgin, R. Agarwal, and V. J. Sorger, Nanophotonics **7**, 455 (2017).
5. Y. Gui, M. Miscuglio, Z. Ma, M. H. Tahersima, S. Sun, R. Amin, H. Dalir, and V. J. Sorger, Sci. Rep. **9**, 11279 (2019).
6. R. Amin, R. Maiti, J. K. George, X. Ma, Z. Ma, H. Dalir, M. Miscuglio, and V. J. Sorger, J. Lightwave Technol. **38**, 282 (2020).
7. N. Kinsey and J. B. Khurgin, Opt. Mater. Express **9**, 2793 (2019).
8. C. Wang, M. Zhang, X. Chen, M. Bertrand, A. Shams-Ansari, S. Chandrasekhar, P. Winzer, and M. Lončar, Nature **562**, 101 (2018).

Table 1. Comparison with Recent Art

Type	$V_\pi L$ (V · μm)	f_{-3dB} (GHz)	IL (dB)	L_d (μm)	V_{bias} (V)	E/bit (fJ)
Thin-film LN [8]	28,000	45	0.4	20,000	2.3	14
LN plasmon [9]	3000	9	5.5	20	50	1,000
EO plasmon [10]	120	70	6	10	12	110
$BaTiO_3$ (BT) [11]	4500	35	14.5	300	2.5	96
EO polymer [12]	–	110	2.5	6	3.3	12
ITO*(This work)	95	1.1	6.7	1.4	20	2046
ITO (Future option)	3	40.2	3.8	1.0	2.2	19

9. M. Thomaschewski, V. A. Zenin, C. Wolff, and S. I. Bozhevolnyi, Nat. Commun. **11**, 748 (2020).
10. M. Ayata, Y. Fedoryshyn, W. Heni, B. Baeuerle, A. Josten, M. Zahner, U. Koch, Y. Salamin, C. Hoessbacher, C. Haffner, D. L. Elder, L. R. Dalton, and J. Leuthold, Science **358**, 630 (2017).
11. S. Abel, F. Eltes, J. E. Ortmann, A. Messner, P. Castera, T. Wagner, D. Urbonas, A. Rosa, A. M. Gutierrez, D. Tulli, P. Ma, B. Baeuerle, A. Josten, W. Heni, D. Caimi, L. Czornomaz, A. A. Demkov, J. Leuthold, P. Sanchis, and J. Fompeyrine, Nat. Mater. **18**, 42 (2019).
12. C. Haffner, D. Chelladurai, Y. Fedoryshyn, A. Josten, B. Baeuerle, W. Heni, T. Watanabe, T. Cui, B. Cheng, S. Saha, D. L. Elder, L. R. Dalton, A. Boltasseva, V. M. Shalaev, N. Kinsey, and J. Leuthold, Nature **556**, 483 (2018).